APPLIED AND ENVIRONMENTAL MICROBIOLOGY, Sept. 2006, p. 5884–5894 Vol. 72, No. 9
0099-2240/06/$08.00+0 doi:10.1128/AEM.00780-06

Quantification of the Effects of Salt Stress and Physiological State on Thermotolerance of *Bacillus cereus* ATCC 10987 and ATCC 14579

Heidy M. W. den Besten,[1,2]* Marios Mataragas,[3] Roy Moezelaar,[1,4] Tjakko Abee,[1,2] and Marcel H. Zwietering[2]

Wageningen Centre for Food Sciences (WCFS), P.O. Box 557, 6700 AN Wageningen, The Netherlands[1]; Wageningen University and Research Centre, Laboratory of Food Microbiology, P.O. Box 8129, 6700 EV Wageningen, The Netherlands[2]; Agricultural University of Athens, Laboratory of Food Quality Control and Hygiene, Iera Odos 75, 118 55 Athens, Greece[3]; and Wageningen University and Research Centre, Food Technology Centre, P.O. Box 17, 6700 AA Wageningen, The Netherlands[4]

Received 4 April 2006/Accepted 16 June 2006

The food-borne pathogen *Bacillus cereus* can acquire enhanced thermal resistance through multiple mechanisms. Two *Bacillus cereus* strains, ATCC 10987 and ATCC 14579, were used to quantify the effects of salt stress and physiological state on thermotolerance. Cultures were exposed to increasing concentrations of sodium chloride for 30 min, after which their thermotolerance was assessed at 50°C. Linear and nonlinear microbial survival models, which cover a wide range of known inactivation curvatures for vegetative cells, were fitted to the inactivation data and evaluated. Based on statistical indices and model characteristics, biphasic models with a shoulder were selected and used for quantification. Each model parameter reflected a survival characteristic, and both models were flexible, allowing a reduction of parameters when certain phenomena were not present. Both strains showed enhanced thermotolerance after preexposure to (non)lethal salt stress conditions in the exponential phase. The maximum adaptive stress response due to salt preexposure demonstrated for exponential-phase cells was comparable to the effect of physiological state on thermotolerance in both strains. However, the adaptive salt stress response was less pronounced for transition- and stationary-phase cells. The distinct tailing of strain ATCC 10987 was attributed to the presence of a subpopulation of spores. The existence of a stable heat-resistant subpopulation of vegetative cells could not be demonstrated for either of the strains. Quantification of the adaptive stress response might be instrumental in understanding adaptation mechanisms and will allow the food industry to develop more accurate and reliable stress-integrated predictive modeling to optimize minimal processing conditions.

Bacillus cereus is a spore-forming gram-positive rod causing both food spoilage and food poisoning. The organism is ubiquitous in soil, in spices, on grass, in dairy cattle feed, and in dung and is an inevitable low-grade contaminant of pasteurized milk products (15). Toxins produced by vegetative cells of *B. cereus* can be the causative agents of two types of gastrointestinal disease, i.e., emesis and diarrhea. The diarrheal type is caused by heat-labile enterotoxins produced in the intestine, whereas emetic outbreaks are associated with the heat-stable cereulide toxin produced in the food product (8).

Consumer demand for mildly processed foods challenges the food industry to produce tasty, nutritious, and microbially safe minimally processed products (16). A minimally processed food product is microbially stable and safe because of the presence of a set of preservation hurdles that is specific for the particular food. An appropriate combination of preservation hurdles controls microbial spoilage and the growth of pathogenic microorganisms and stabilizes the sensory and nutritive properties of a food. During processing, microorganisms in the food undergo various kinds of stresses, and these stresses have a fundamental impact on the behavior of the stress-exposed cells. Bacteria have evolved adaptive networks to face the challenges of changing environments (1). Upon triggering of the adaptive networks, the so-called adaptive stress response, the bacteria gain increased resistance towards conditions which would be lethal for the cells if the stress response was not activated. This is of practical importance for minimally processed foods, as the adaptive stress response to the first hurdle may render the organism more resistant to the subsequent hurdle(s). Therefore, the adaptive stress response may counterbalance the benefits of the hurdle concept.

The effect of stress preexposure on thermotolerance of vegetative cells of *B. cereus* has been investigated previously (4, 22, 28). However, in most investigations, thermotolerance was assessed in exponentially growing cultures after preexposure to just one condition per stress-inducing factor, and the end-point method was used to evaluate the effect of stress preexposure on thermotolerance. The main disadvantage of the end-point method is that it does not provide information on the thermal death kinetics, which could provide valuable knowledge for quantitative risk assessment studies and might reflect the mechanisms by which stress preexposure influences thermotolerance. In the last decades, a number of mathematical primary models have been developed to quantitatively describe microbial inactivation. Primary kinetic models describe microbial survival as a function of time. An important aspect of modeling is the possibility of reliable estimation of the effects of various stress conditions on the number of surviving microorganisms. Therefore, in this study we evaluated the fitting performance of different primary models, which cover a wide range of inactivation curvatures for vegetative cells. The most suitable models were selected in order to identify the survival curvature characteristics in more detail and to quantify the effects of the adaptive stress response and physiological state on the inactivation kinetics.

* Corresponding author. Mailing address: Wageningen University and Research Centre, Laboratory of Food Microbiology, P.O. Box 8129, 6700 EV Wageningen, The Netherlands. Phone: 31-317-484977. Fax: 31-317-484978. E-mail: heidy.denbesten@wur.nl.

MATERIALS AND METHODS

Bacterial strains and culture conditions. *Bacillus cereus* ATCC 10987, isolated from a study on cheese spoilage in Canada in 1930 (24), and *Bacillus cereus* ATCC 14579, isolated from the air in a cow shed in the United Kingdom (9), were used in this study. The cultures were stored frozen (−80°C) in brain heart infusion (BHI) broth (Becton Dickinson, France) supplemented with 25% glycerol (Sigma). The bacteria were cultivated before each experiment in 10 ml BHI broth and incubated in a water bath at 30°C with aeration at 200 rpm (Julabo SW20; Julabo Labortechnik GmbH, Germany) for 16 to 24 h.

Thermal inactivation experiments with and without preexposure of cells to salt. To evaluate the effects of preexposure to salt and of physiological state on thermotolerance, the following procedure was used. Erlenmeyer flasks (250 ml) with 50 ml of sterile BHI broth were inoculated with an overnight culture to reach an optical density (OD) of approximately 0.025 at 600 nm (Novaspec II spectrophotometer; Pharmacia Biotech, United Kingdom). The flasks were incubated in a water bath at 30°C with aeration at 200 rpm until a specific OD value was reached, depending on the desired physiological state (exponential phase, OD = 0.5; transition phase, OD = 5; stationary phase, OD = 10 to 12). Cells were harvested by centrifugation of 20 ml of culture (3,660 × *g*, 5 min, 20°C) (Mistral 3000i; MSE, United Kingdom), and the supernatant was removed immediately after centrifugation. To preexpose the harvested cells to salt, the cells were resuspended in 20 ml BHI broth containing sodium chloride (VWR-International, France) at various concentrations (final concentrations of sodium chloride were as follows: for exponential-phase cells, 1%, 2.5%, and 5%; and for transition- and stationary-phase cells, 2.5% [wt/vol]) and incubated for 30 min in a water bath (30°C, 200 rpm). After preexposure to salt, the cells were spun down and resuspended in 2 ml BHI broth. When cells were not preexposed to sodium chloride, 20 ml of culture was centrifuged and concentrated in 2 ml BHI broth.

To inactivate the (non)preexposed cells, six tubes (Greiner Bio-One, Germany) containing 20 ml of preheated BHI broth were placed in a water bath (GFL 1083; Gesellschaft Labortechnik GmbH, Germany) with aeration (150 rpm). The desired temperature (50°C) of the preheated BHI broth was checked with a digital thermometer (TFX 392 SK; Gullimex Instruments, Germany). From the concentrated culture, 200 μl was inoculated into each tube. At constant intervals, 1-ml samples were taken in duplicate, and serial dilutions were made in 9 ml peptone saline solution (1 g neutralized bacteriological peptone [Oxoid, United Kingdom] supplemented with 8.5 g sodium chloride per liter). From the appropriate dilution, 50 μl was spread in duplicate on BHI agar plates (BHI broth supplemented with 15 g agar [Oxoid, United Kingdom] per liter) by use of a spiral plater (Eddy Jet; IUL Instruments, Spain). Plates were incubated at 30°C for 24 h, and the results were expressed in $\log_{10}$ CFU ml^{-1} (detection limit of the method, 1.3 $\log_{10}$ CFU ml^{-1}). For all experimental conditions, three experiments were performed on different days.

Microbial survival models. The following models were used to fit the inactivation data.

(i) The first-order model (31) was determined with the following equation:

$$\log_{10} N(t) = \log_{10} N(0) - \frac{t}{D} \quad (1)$$

where D is the decimal reduction time, which is the time needed for 1 $\log_{10}$ reduction of the population (min); $N(0)$ is the initial population ($\log_{10}$ CFU ml^{-1}); and $N(t)$ is the population at time t ($\log_{10}$ CFU ml^{-1}).

(ii) The Weibull model (7) was determined with the following equation:

$$\log_{10} N(t) = \log_{10} N(0) - \left(\frac{t}{\delta}\right)^{\beta} \quad (2)$$

where δ is the first decimal reduction time (min) and β is a fitting parameter which defines the shape of the curve. β values of <1 correspond to concave upward survival curves, β values of >1 correspond to concave downward curves, and a β value of 1 corresponds to a straight line (same as equation 1).

(iii) The biphasic linear model, or two-population model, was proposed by Cerf. The biphasic model assumes the existence of two populations, with one heat-sensitive and one heat-resistant population (6). The biphasic linear model can be formulated as follows:

$$\log_{10} N(t) = \log_{10} N(0) + \log_{10}\left[(1-f)\cdot 10^{-\frac{t}{D_{sens}}} + f\cdot 10^{-\frac{t}{D_{res}}}\right] \quad (3)$$

where $(1 - f)$ and f are the fractions of the heat-sensitive and heat-resistant populations, respectively, and D_{sens} and D_{res} are the decimal reduction times of the two populations, respectively (min).

(iv) The biphasic logistic model (30) assumes the existence of a primary heat-sensitive population and a secondary heat-resistant population and aims to take into account a shoulder for both populations. The biphasic logistic model is formulated as follows:

$$\log_{10} N(t) = \log_{10} N(0) + \log_{10} \times \left\{\frac{(1-f)\cdot[1+\exp(-k_{sens}\cdot t_s)]}{1+\exp[k_{sens}\cdot(t-t_s)]} + \frac{f\cdot[1+\exp(-k_{res}\cdot t_s)]}{1+\exp[k_{res}\cdot(t-t_s)]}\right\} \quad (4)$$

where t_s is the duration of the shoulder (min), $(1 - f)$ and f are the fractions of the heat-sensitive and heat-resistant populations, respectively, and k_{sens} and k_{res} are the maximum specific inactivation rates for the heat-sensitive and heat-resistant populations, respectively (min^{-1}). The respective decimal reduction times can be calculated from the inactivation rates by the equation $D = \ln(10)/k$. When no shoulder or second population is present, then $t_s = 0$ or $f = 0$, respectively.

(v) The modified Gompertz model (27) was determined with the following equation:

$$\log_{10} N(t) = \log_{10} N(0) + a\cdot\exp[-\exp(b + c\cdot t)] - a\cdot\exp[-\exp(b)] \quad (5)$$

where a, b, and c are fitting parameters.

(vi) The reparameterized Gompertz model, as modified by Zwietering et al. (33), was determined with the following equation:

$$\log_{10} N(t) = \log_{10} N(0) + A\cdot\exp\left\{-\exp\left[\frac{k\cdot e}{-A}\cdot(t_s - t) + 1\right]\right\} \quad (6)$$

where t_s is the duration of the shoulder (min), k is the maximum specific inactivation rate ($\log_{10}$ min^{-1}), and A is the difference between the population at the end of the inactivation period and the initial population ($\log_{10}$ CFU ml^{-1}).

(vii) The Baranyi model was proposed by Baranyi et al. (2) and considers an inactivation curve as the mirror image of a growth curve. The Baranyi growth model can be written with the following equations (with $m = 1$ and $\upsilon = \mu$) (2):

$$\log_{10} N(t) = \log_{10} N(0) + \frac{\mu}{\ln(10)}\cdot A(t) - \frac{1}{\ln(10)}\cdot\ln\left\{1 + \frac{\exp[\mu\cdot A(t)] - 1}{10^{[\log_{10} N(\text{final}) - \log_{10} N(0)]}}\right\} \quad (7a)$$

where μ is the maximum specific growth rate (min^{-1}), $N(final)$ is the final population ($\log_{10}$ CFU ml^{-1}), and $A(t)$ is as defined by Baranyi et al. (2).

$$A(t) = t + \frac{1}{\mu}\cdot\ln[\exp(-\mu\cdot t) + \exp(-\mu\cdot t_{lag}) - \exp(-\mu\cdot t - \mu\cdot t_{lag})] \quad (7b)$$

where t_{lag} is the duration of the lag period of the growth curve (min).

(viii) The Geeraerd model assumes that the total population N equals the sum of two subpopulations, with one of them having more heat resistance ($N = N_{sens} + N_{res}$) (11). Inactivation of cells ensues when a critical component (C_c) is inactivated or destructed. The following equations define the model:

$$\frac{dN_{sens}(t)}{dt} = -k_{sens}\cdot N_{sens}(t)\cdot\left[\frac{1}{1+C_c(t)}\right] \quad (8a)$$

$$\frac{dN_{res}(t)}{dt} = -k_{res}\cdot N_{res}(t)\cdot\left[\frac{1}{1+C_c(t)}\right] \quad (8b)$$

$$\frac{dC_c(t)}{dt} = -k_{sens}\cdot C_c(t) \quad (8c)$$

where $C_c(0) = \exp(k_{sens}\cdot t_s) - 1$.

The solution of this set of differential equations can be expressed as follows (11; A. H. Geeraerd, personal communication):

$$\log_{10} N(t) = \log_{10} N(0) + \log_{10} \times \left\{(1-f)\cdot\exp(-k_{sens}\cdot t)\cdot\frac{\exp(k_{sens}\cdot t_s)}{1+[\exp(k_{sens}\cdot t_s)-1]\cdot\exp(-k_{sens}\cdot t)} + f\cdot\exp(-k_{res}\cdot t)\cdot\left(\frac{\exp(k_{sens}\cdot t_s)}{1+[\exp(k_{sens}\cdot t_s)-1]\cdot\exp(-k_{sens}\cdot t)}\right)^{\frac{k_{res}}{k_{sens}}}\right\} \quad (9)$$

where t_s is the duration of the shoulder (min), $(1 - f)$ and f are the fractions of

the heat-sensitive and heat-resistant populations, respectively, and k_{sens} and k_{res} are the maximum specific inactivation rates of the heat-sensitive and heat-resistant populations, respectively (min^{-1}).

Model fitting and model selection. The above models were fitted to the inactivation data per the experimental conditions in TableCurve 2D (Windows v. 2.03) and checked in Microsoft Excel by using the Excel Solver add-in. The Baranyi growth model was fitted to the mirror image of the inactivation data points in TableCurve following the procedure suggested by Baranyi et al. (2), and the freeware MicroFit 1.0 (Institute of Food Research, Norwich, United Kingdom) was used to check the TableCurve fitting results when the experimental data set was limited to 100 data points.

The criteria used to select the most adequate model to fit the experimental data were as follows: applicability for both strains ATCC 10987 and ATCC 14579 and the different experimental conditions, statistics (MSE_{model}, r^2, A_f, and F test), biological meaning of the parameters, and reflection of a proposed inactivation mechanism.

The statistical indices used to compare the models are discussed below (26).

(i) MSE_{model}. The mean square error of the model (MSE_{model}) is the residual sum of squares (sum of the squared differences between the observed values and the fitted values) divided by the degrees of freedom. The lower the MSE_{model} is, the better is the adequacy of the model to describe the data. It was calculated by the following equation:

$$MSE_{model} = \frac{RSS}{DF} = \frac{\sum_{i=1}^{n} (\log_{10} N^i_{observed} - \log_{10} N^i_{fitted})^2}{n - s} \quad (10)$$

where RSS is the residual sum of squares, DF is the degrees of freedom, n is the number of data points, s is the number of parameters of the model, $N^i_{observed}$ is the observed population level ($\log_{10}$ CFU ml^{-1}), and N^i_{fitted} is the fitted population level ($\log_{10}$ CFU ml^{-1}).

(ii) r^2. The regression coefficient (r^2) is the proportion of the total variation of the data explained by the model. The value can range between 0 and 1, and the higher the value, the better the fit of the model. r^2 was calculated by the following equation:

$$r^2 = 1 - \frac{RSS}{TSS} \quad (11)$$

where RSS is the residual sum of squares and TSS is the total sum of squares, which is the total amount of variation present when the observed values are compared to the grand average of the observed values.

(iii) A_f. The accuracy factor (A_f) shows the accuracy of the model and indicates how close the fitted values are, on average, to the observed values. The larger the value, the less accurate the model, and when A_f is equal to 1, there is perfect agreement between the fitted and the observed values. An A_f of 2 indicates that the fitted values are, on average, different by a factor of 2 from the observed values (i.e., either half as large or twice as large). The A_f was calculated by the following equation:

$$A_f = 10^{\left[\sum_{i=1}^{n} |\log_{10}(\log_{10} N^i_{fitted} / \log_{10} N^i_{observed})| / n \right]} \quad (12)$$

where n is the number of data points.

(iv) F test. The F test was used to decide if the fitting performance of a model was statistically accepted. The f value was calculated by the following equation:

$$f = \frac{MSE_{model}}{MSE_{data}} \quad (13)$$

where MSE_{model} is the mean square error of the model and MSE_{data} is the mean square error of the data for replicate values, which indicates the measuring error. MSE_{data} was determined by the deviation of the observed values from the mean value at one time point, i, and was calculated as follows:

$$MSE_{data} = \frac{RSS}{DF} = \frac{\sum_{i=1}^{m} \sum_{j=1}^{k} (\text{average } \log_{10} N^i - \log_{10} N^{ij})^2}{n - m} \quad (14)$$

where n is the number of data points, m is the number of time points (sampling times), k is the number of replicates at each time point, average N^i is the mean value of the population at time point i ($\log_{10}$ CFU ml^{-1}), and N^{ij} is the population at time point i for specific replicate j ($\log_{10}$ CFU ml^{-1}).

The f value was tested against an F table value (95% confidence). If the f value was smaller than the F table value ($F^{DF_{model}}_{DF_{data}}$), then the F test was accepted, and this indicated that the model described the observed data well.

Reduction of model parameters. After selection of the most adequate model(s) for fitting the data using the criteria mentioned above, a stepwise procedure was followed in order to reduce, where possible, the number of parameters of the selected model per experimental condition. The selected model was fitted to all the replicate data together per experimental condition, and the confidence interval (95%) of the parameter estimate was used to evaluate whether a parameter could be excluded from the model. If the confidence interval (95%) of the parameter estimate included zero, the parameter was regarded as nonsignificant. After the exclusion of a nonsignificant parameter, the model with the reduced number of parameters was refitted to the data to check for another nonsignificant parameter, which was subsequently excluded as well. The stepwise procedure was followed until only the significant parameters remained in the model. However, due to the reduction of parameters, there was a risk that the reduced model failed to describe the data acceptably. This can be the case if by reducing one parameter, a second parameter also becomes redundant. Therefore, the F test was applied each time after the exclusion of one nonsignificant parameter to evaluate if the reduction of parameters was still statistically acceptable (33). If the F test was not accepted, the model reduction was not performed regardless of whether a nonsignificant parameter was included in the model. The f value to test if a parameter could be excluded was calculated by the following equation:

$$f = \frac{(RSS_2 - RSS_1)/(DF_2 - DF_1)}{RSS_1/DF_1} \quad (15)$$

where RSS_1 is the residual sum of squares of the full model, RSS_2 is the residual sum of squares of the reduced model, and DF_1 and DF_2 are the degrees of freedom for the full and reduced models, respectively, calculated by the formula DF = number of data points − number of parameters.

The f value was tested against an F table value (95% confidence, $F^{DF_2 - DF_1}_{DF_1}$). If the f value was smaller than the F table value, the F test was accepted and the nonsignificant parameter was excluded from the model.

Statistical analysis of model parameters. For all experimental conditions, three independent experiments were performed on different days, and the selected, reduced model was fitted to the reproductions individually. One-way analysis of variance and t tests (one-sided) were performed in order to compare the average parameter estimates for the different conditions and to investigate if there were any significant effects of preexposure to salt and of physiological state on the inactivation kinetic parameters (SPSS, version 11.5.0).

RESULTS

To select the sodium chloride concentrations for salt preexposure, the growth of *B. cereus* ATCC 10987 and ATCC 14579 was determined in BHI broth supplemented with 1%, 2.5%, 5%, and 10% sodium chloride (wt/vol) for 300 min. The two *B. cereus* strains were able to grow in the presence of salt in the growth medium (1% and 2.5%), although exposure to 2.5% sodium chloride resulted in an initial decline in the number of cells. Higher salt concentrations (5% and 10%) proved to be lethal for the bacterial cells (data not shown). The concentrations of 1%, 2.5%, and 5% sodium chloride were chosen in order to investigate the effects of preexposure to nonlethal and lethal salt conditions on thermotolerance.

Effects of salt stress and physiological state on thermotolerance: strain diversity and population heterogeneity. Figure 1 illustrates the influences of preexposure to salt and physiological state on thermotolerance at 50°C for *B. cereus* ATCC 10987 (panel a) and ATCC 14579 (panel b). The thermotolerance of exponential-phase cells of both strains was highly increased by preexposure to 1%, 2.5%, and 5% sodium chloride, resulting in a lower inactivation rate for strain ATCC

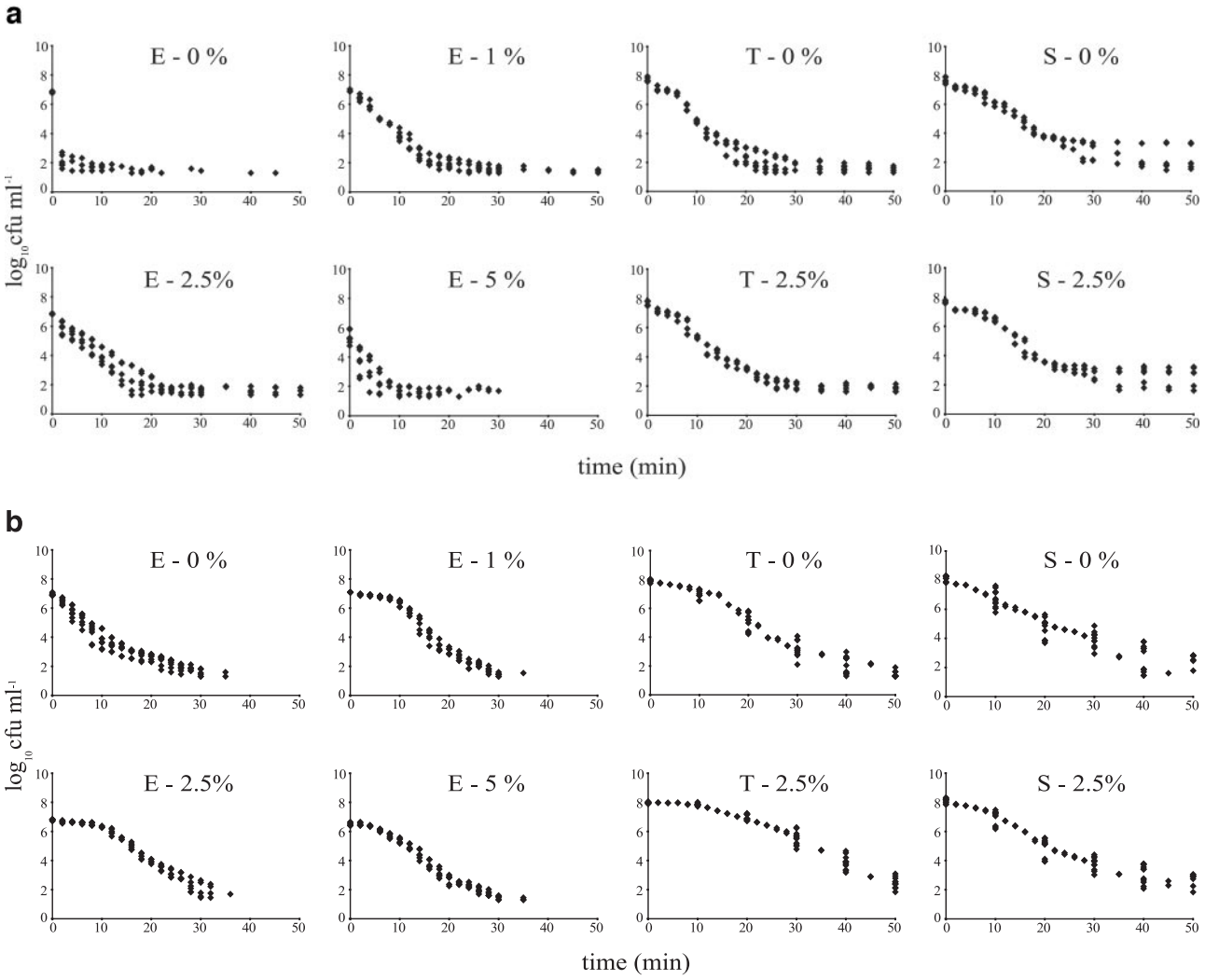

FIG. 1. (a) Thermal inactivation of *Bacillus cereus* ATCC 10987 cells at 50°C with(out) preexposure to sodium chloride for 30 min (sodium chloride concentrations for exponential [E]-phase cells, 1%, 2.5%, and 5%; sodium chloride concentration for transition [T]- and stationary [S]-phase cells, 2.5% [wt/vol]). The detection limit was 1.3 $\log_{10}$ CFU ml^{-1}. (b) Thermal inactivation of *Bacillus cereus* ATCC 14579 cells at 50°C with(out) preexposure to sodium chloride for 30 min (sodium chloride concentrations for exponential-phase cells, 1%, 2.5%, and 5%; sodium chloride concentration for transition- and stationary-phase cells, 2.5% [wt/vol]). The detection limit was 1.3 $\log_{10}$ CFU ml^{-1}.

10987 compared to the experimental condition without preexposure to salt and an additional shoulder period for strain ATCC 14579. Preexposure to 1% and 2.5% salt seemed to be most effective. The observed shoulder for strain ATCC 14579 after preexposure to salt could not be dismissed as an experimental artifact of cell clumping. Wet mounts of cell suspensions collected at the start of the inactivation showed no aggregation.

Both strains demonstrated a growth cycle-dependent effect on thermotolerance. Transition- and stationary-phase cells exhibited more resistance to heat than exponential-phase cells. The adaptive stress response was also influenced by physiological state; the effect of preexposure to salt on thermotolerance was less pronounced for transition- and stationary-phase cells than for exponential-phase cells for both strains.

Strain ATCC 10987 showed distinct tailing in the exponential, transition, and stationary phases (Fig. 1a), indicating the presence of a highly heat-resistant subpopulation. To investigate the potential presence of spores in very small numbers at the start of inactivation, suspensions from the three growth phases were heated for 15 min at 75°C to kill the vegetative cells. The observed tailing was indeed explained by minor fractions of spores present in the suspensions at the start of the inactivation, since the subpopulation detected after heating at 75°C corresponded to the tailing fraction. The presence of spores in the exponentially growing culture could be explained by the transfer of spores from the overnight culture during inoculation of the fresh medium. Germination of spores during incubation to exponential growth phase was apparently limited. The failure of these spores to germinate was not investigated any further. Strain ATCC 14579 was also able to form spores in the stationary phase, but the fraction of spores was very small, such that no spores could be detected at the start of inactivation.

Assessment of model adequacy and model selection. The inactivation kinetics of the two *B. cereus* strains studied were

TABLE 1. Statistical indices of microbial survival models used for fitting the inactivation data for *Bacillus cereus* strains ATCC 10987 and ATCC 14579

Strain, growth phase, and % NaCl	Statistical index	Statistical index value (no. of model parameters)							
		Linear (2)	Weibull (3)	Biphasic linear (4)	Biphasic logistic (5)	Modified Gompertz (4)	Reparameterized Gompertz (4)	Baranyi (4)	Geeraerd (5)
ATCC 10987									
Exponential									
0	r^2	0.2284	0.9022	0.9798	0.9796	0.9756	0.9753	0.9751	0.9798
	A_f	1.62	1.34	1.11	1.11	1.13	1.13	1.13	1.11
	MSE_{model}	2.5136	0.3746	0.0689	0.0712	0.0832	0.0842	0.0849	0.0706
	F	28.32	4.22	**0.78**	**0.80**	**0.94**	**0.95**	**0.96**	**0.80**
	F table	1.78	1.78	1.78	1.79	1.78	1.78	1.78	1.79
1	r^2	0.6788	0.8696	0.9816	0.9818	0.9809	0.9809	0.9789	0.9819
	A_f	1.44	1.33	1.09	1.09	1.09	1.09	1.10	1.09
	MSE_{model}	1.1110	0.4555	0.0648	0.0648	0.0673	0.0673	0.0744	0.0645
	F	12.52	5.13	**0.73**	**0.73**	**0.76**	**0.76**	**0.84**	**0.73**
	F table	1.41	1.41	1.41	1.41	1.41	1.41	1.41	1.41
2.5	r^2	0.6826	0.8546	0.9448	0.9449	0.9409	0.9409	0.9455	0.9458
	A_f	1.43	1.29	1.14	1.13	1.14	1.14	1.13	1.13
	MSE_{model}	0.9873	0.4567	0.1750	0.1771	0.1875	0.1875	0.1728	0.1737
	F	5.16	2.39	**0.91**	**0.93**	**0.98**	**0.98**	**0.90**	**0.91**
	F table	1.41	1.41	1.41	1.41	1.41	1.41	1.41	1.41
5	r^2	0.5024	0.7907	0.8489	0.8488	0.8550	0.8551	0.8592	0.8590
	A_f	1.43	1.24	1.17	1.17	1.17	1.17	1.16	1.16
	MSE_{model}	0.9242	0.3947	0.2895	0.2944	0.2777	0.2776	0.2697	0.2743
	F	2.91	**1.24**	**0.91**	**0.93**	**0.88**	**0.87**	**0.85**	**0.86**
	F table	1.55	1.56	1.56	1.56	1.56	1.56	1.56	1.56
Transition									
0	r^2	0.7368	0.8654	0.9662	0.9680	0.9717	0.9717	0.9661	0.9682
	A_f	1.42	1.35	1.14	1.14	1.13	1.13	1.13	1.14
	MSE_{model}	1.2524	0.6458	0.1638	0.1560	0.1369	0.1369	0.1640	0.1554
	F	9.18	4.73	**1.20**	**1.14**	**1.00**	**1.00**	**1.20**	**1.14**
	F table	1.38	1.38	1.38	1.38	1.38	1.38	1.38	1.38
2.5	r^2	0.7990	0.9045	0.9820	0.9823	0.9853	0.9853	0.9808	0.9824
	A_f	1.42	1.21	1.07	1.07	1.06	1.06	1.07	1.07
	MSE_{model}	0.8106	0.3887	0.0738	0.0731	0.0605	0.0605	0.0787	0.0728
	F	15.22	7.30	1.39	**1.37**	**1.14**	**1.14**	1.48	**1.37**
	F table	1.38	1.38	1.38	1.38	1.38	1.38	1.38	1.38
Stationary									
0	r^2	0.7946	0.8926	0.9548	0.9570	0.9569	0.9569	0.9481	0.9572
	A_f	1.35	1.19	1.11	1.11	1.11	1.11	1.13	1.11
	MSE_{model}	0.7952	0.4188	0.1775	0.1703	0.1692	0.1692	0.2041	0.1696
	F	4.58	2.41	**1.02**	**0.98**	**0.97**	**0.97**	**1.18**	**0.98**
	F table	1.35	1.35	1.35	1.35	1.35	1.35	1.35	1.35
2.5	r^2	0.7037	0.8355	0.9462	0.9590	0.9572	0.9572	0.9499	0.9592
	A_f	1.34	1.22	1.12	1.11	1.11	1.11	1.12	1.11
	MSE_{model}	1.1115	0.6219	0.2051	0.1575	0.1632	0.1632	0.1910	0.1566
	F	6.80	3.81	**1.26**	**0.96**	**1.00**	**1.00**	**1.17**	**0.96**
	F table	1.36	1.36	1.36	1.36	1.36	1.36	1.36	1.36
Goodness of fit[a]		0/8	1/8	7/8	8/8	8/8	8/8	7/8	8/8
ATCC 14579									
Exponential									
0	r^2	0.8821	0.9413	0.9615	0.9621	0.9575	0.9576	0.9407	0.9622
	A_f	1.18	1.11	1.09	1.09	1.10	1.09	1.12	1.09
	MSE_{model}	0.3326	0.1671	0.1105	0.1096	0.1221	0.1218	0.1703	0.1095
	F	2.83	1.42	**0.94**	**0.93**	**1.04**	**1.04**	1.45	**0.93**
	F table	1.37	1.37	1.37	1.37	1.37	1.37	1.37	1.37
1	r^2	0.9455	0.9496	0.9455	0.9869	0.9870	0.9870	0.9829	0.9869
	A_f	1.12	1.11	1.12	1.06	1.06	1.06	1.07	1.06
	MSE_{model}	0.2436	0.2274	0.2489	0.0604	0.0592	0.0592	0.0781	0.0604
	F	4.46	4.17	4.56	**1.11**	**1.08**	**1.08**	**1.43**	**1.11**
	F table	1.43	1.43	1.43	1.43	1.43	1.43	1.43	1.43
2.5	r^2	0.9459	0.9647	0.9459	0.9833	0.9833	0.9833	0.9831	0.9833
	A_f	1.10	1.09	1.10	1.06	1.06	1.06	1.06	1.06
	MSE_{model}	0.1761	0.1163	0.1800	0.0563	0.0556	0.0556	0.0561	0.0563
	F	3.16	2.09	3.24	**1.01**	**1.00**	**1.00**	**1.01**	**1.01**
	F table	1.45	1.45	1.45	1.45	1.45	1.45	1.45	1.45

Continued on following page

TABLE 1—*Continued*

Strain, growth phase, and % NaCl	Statistical index	Statistical index value (no. of model parameters)							
		Linear (2)	Weibull (3)	Biphasic linear (4)	Biphasic logistic (5)	Modified Gompertz (4)	Reparameterized Gompertz (4)	Baranyi (4)	Geeraerd (5)
5	r^2	0.9612	0.9613	0.9740	0.9886	0.9890	0.9890	0.9862	0.9886
	A_f	1.12	1.12	1.07	1.05	1.05	1.05	1.06	1.05
	MSE_{model}	0.1346	0.1358	0.0919	0.0408	0.0390	0.0390	0.0490	0.0408
	F	3.59	3.63	2.45	**1.09**	**1.04**	**1.04**	**1.31**	**1.09**
	F table	1.42	1.43	1.43	1.43	1.43	1.43	1.43	1.43
Transition									
0	r^2	0.9412	0.9445	0.9412	0.9744	0.9753	0.9753	0.9712	0.9744
	A_f	1.17	1.15	1.17	1.10	1.10	1.10	1.11	1.10
	MSE_{model}	0.3456	0.3297	0.3530	0.1556	0.1485	0.1485	0.1728	0.1556
	F	2.23	2.12	2.28	**1.00**	**0.96**	**0.96**	**1.11**	**1.00**
	F table	1.44	1.44	1.44	1.44	1.44	1.44	1.44	1.44
2.5	r^2	0.9307	0.9764	0.9307	0.9792	0.9809	0.9809	0.9801	0.9792
	A_f	1.09	1.05	1.09	1.05	1.04	1.04	1.04	1.05
	MSE_{model}	0.2679	0.0923	0.2739	0.0856	0.0754	0.0754	0.0786	0.0844
	F	3.06	**1.06**	3.13	**0.98**	**0.86**	**0.86**	**0.90**	**0.97**
	F table	1.45	1.45	1.45	1.45	1.45	1.45	1.45	1.45
Stationary									
0	r^2	0.8956	0.9176	0.8956	0.9303	0.9307	0.9307	0.9277	0.9303
	A_f	1.14	1.15	1.14	1.12	1.12	1.12	1.13	1.12
	MSE_{model}	0.4492	0.3587	0.4596	0.3106	0.3051	0.3051	0.3181	0.3106
	F	**1.42**	**1.13**	**1.45**	**0.98**	**0.96**	**0.96**	**1.00**	**0.98**
	F table	1.47	1.47	1.47	1.47	1.47	1.47	1.47	1.47
2.5	r^2	0.9173	0.9340	0.9173	0.9597	0.9560	0.9560	0.9475	0.9597
	A_f	1.14	1.11	1.14	1.09	1.09	1.09	1.10	1.09
	MSE_{model}	0.3495	0.2819	0.3572	0.1761	0.1902	0.1902	0.2268	0.1761
	F	1.82	1.46	1.86	**0.91**	**0.99**	**0.99**	**1.18**	**0.91**
	F table	1.45	1.45	1.45	1.46	1.45	1.45	1.45	1.46
Goodness of fit[a]		1/8	2/8	2/8	8/8	8/8	8/8	7/8	8/8

[a] For the goodness of fit, 0/8 indicates that the model was accepted for none of the eight experimental conditions, and 8/8 indicates that the model was accepted for all experimental conditions. Bold values indicate that the F test was accepted.

further analyzed by fitting eight microbial survival models to the experimental data. The fitting performances of these models were assessed statistically and evaluated in order to select the most suitable model(s) to quantify in more detail specific curvature characteristics and to quantify the effects of preexposure to salt and of growth phase on thermotolerance.

To compare the fitting performances of the models, MSE_{model}, r^2, A_f, and the f value were calculated (Table 1). Comparison of the indices of the models showed that overall, the first-order model and the Weibull model did not describe the inactivation data for strains ATCC 10987 and ATCC 14579 acceptably, and neither did the biphasic linear model for the latter strain, which could be confirmed by the F test. When the F test was accepted (bold values), this indicated that the model described the observed inactivation data well. The rejection of the biphasic linear model for strain ATCC 14579 was caused by the inability of this model to describe the shoulder curvature. The Baranyi model was statistically acceptable for most of the experimental conditions, except for transition-phase cells of strain ATCC 10987 with preexposure to 2.5% salt and exponential-phase cells of strain ATCC 14579 without preexposure to salt. One of the noticeable differences between the Baranyi model and other sigmoid curves, such as the modified Gompertz model, is that the mid-phase of the model curvature is very close to linear. This property of the Baranyi model was not applicable for exponential-phase cells of strain ATCC 14579 without preexposure to salt, as this condition showed a nonconstant inactivation rate in the mid-phase.

The statistical indices of the modified Gompertz model, the reparameterized Gompertz model, the biphasic logistic model, and the Geeraerd model were similar in being accepted statistically for all experimental conditions. To choose the most suitable of these remaining models, the following criteria were used: biological meaning of the parameters and reflection of a proposed inactivation mechanism. The modified Gompertz model contains mathematical parameters which have no biological interpretation. Reparameterization, resulting in the reparameterized Gompertz model, replaces the mathematical parameters with parameters that have biological meaning. As expected, the two Gompertz models gave similar statistical indices. The term $a \cdot \exp[-\exp(b)]$ is disregarded in the reparameterized modified Gompertz model, and the effect of this model reduction on the statistical indices was negligible. Parameter A of the reparameterized Gompertz model represents the difference between the population at the end of the observation and the initial population and might reflect a highly resistant subpopulation present in the tail of the sigmoid curvature. The latter phenomenon was applicable for strain ATCC 10987 since the presence of spores was confirmed. The reparameterized Gompertz model did not reflect the population heterogeneity for strain ATCC 14579 suitably, as this strain did not show distinct tailing caused by a subpopulation of cells for which the inactivation rate was equal to zero. In addition, description of a curvature without a tail (linear inactivation or linear inactivation with shoulder) using the reparameterized Gompertz model resulted in a nonrealistic esti-

TABLE 2. Parameter estimates of the biphasic logistic model

Strain	Growth phase	% NaCl	Parameter value[c]				
			$\log_{10} N(0)$	f	k_{sens}	t_S	k_{res}
ATCC 10987	Exponential	0	6.85	5.94×10^{-6}	6.00	NS	0[a]
		1	6.84	6.10×10^{-6}	0.74	NS	0[a]
		2.5	6.48	1.54×10^{-5}	0.65	NS	0[a]
		5	5.04	4.59×10^{-4}	1.18	NS	0[a]
	Transition	0	7.74	9.42×10^{-7}	0.69	NS	0[a]
		2.5	7.61	2.48×10^{-6}	0.57	NS	0[a]
	Stationary	0	7.56	3.94×10^{-6}	0.43	NS	0[a]
		2.5	7.39	1.72×10^{-5}	0.61	5.63	0[a]
ATCC 14579	Exponential	0	6.96	1.65×10^{-3}	0.84	NS	0.22
		1	6.92	1.19×10^{-3}[b]	0.91	8.86	0.27
		2.5	6.70	2.89×10^{-4}[b]	0.57	9.05	0.14[b]
		5	6.49	5.66×10^{-4}[b]	0.63	5.84	0.17
	Transition	0	7.86	6.30×10^{-5}[b]	0.47	6.66	0.12
		2.5	7.95	NS	0.35	13.50	NS
	Stationary	0	8.04	3.63×10^{-4}[b]	0.38	NS	0.12
		2.5	8.07	1.41×10^{-3}[b]	0.49	5.02	0.15

[a] Parameter was fixed at 0 because the inactivation rate k_{res} was 0 for the heat-resistant population of spores at 50°C.
[b] Parameter was not significant for this experimental condition, but the parameter was not excluded from the model because the F test showed that the phenomenon of two populations was significant.
[c] NS, nonsignificant parameter for this experimental condition.

mation of parameter A. Therefore, the two sigmoid models were not regarded as adequate, although the number of parameters was less (four parameters) than that for the biphasic logistic model and the Geeraerd model (five parameters). The biphasic logistic model and the Geeraerd model assume the presence of a primary heat-sensitive and a secondary heat-resistant population, and both models include a shoulder period (t_s). The parameters of the biphasic logistic and Geeraerd model can be given biological meaning, have clear significance, and can be recognized easily in the inactivation curvature. Moreover, both models are flexible, allowing a decrease in the number of parameters when certain phenomena are not present. The biphasic logistic model is derived from a logistic-based model. The Geeraerd model is based on the interesting features of a dynamic model and addresses the hypothesis of the presence of a pool of protective or critical components (C_c) around or in each cell (10, 11). Gradually, this pool is destroyed, undergoing first-order inactivation, and becomes approximately zero. Towards this time, the heat-sensitive and heat-resistant populations are inactivated following first-order kinetics. Taking into account these aspects, the Geeraerd model was considered the most adequate model. The dynamic properties of this model and the underlying hypothesis about the occurrence of a shoulder in an inactivation curve were preferred over the logistic-based properties of the biphasic logistic model. However, both the biphasic logistic and Geeraerd models were used to quantify the effects of salt stress and growth phase on thermotolerance, as both models were able to fit the inactivation characteristics occurring for strains ATCC 10987 and ATCC 14579 suitably.

Reduction of model parameters. The number of parameters of the selected biphasic logistic and Geeraerd models was reduced, where possible, to decrease the model complexity. A stepwise procedure was followed, and the F test was used to determine whether the reduction of parameters was acceptable. Because the tailing fraction for the three physiological growth phases of strain ATCC 10987 corresponded to a minor population of spores, the inactivation rate of the heat-resistant subpopulation (k_{res}) was set at zero, resulting in a four-parameter model before the stepwise procedure was applied for this strain. It should be noted that the fixation of parameter k_{res} at zero resulted in a nonaccepted F test for one experimental condition (transition phase with preexposure to 2.5% salt) for the biphasic logistic and Geeraerd models. The measuring error for this experimental condition was very small (MSE_{data} = 0.05), as replicate experiments produced small variation. Visual inspection of the fitting performances of the biphasic logistic and Geeraerd models showed that the adequacies of both models were sufficient, although the F test was not accepted due to the low MSE_{data}. Tables 2 and 3 show the parameter estimates obtained with the reduced biphasic logistic and reduced Geeraerd models. The numbers of parameters of the reduced biphasic logistic and reduced Geeraerd models were similar, except for one experimental condition for strain ATCC 10987 (transition phase without preexposure to salt). For this condition, parameter t_s was not significant for the biphasic logistic model ($P = 0.12$) but was significant for the Geeraerd model ($P = 0.01$).

Strain ATCC 10987 showed a significant fraction, f, of heat-resistant cells for the various experimental conditions, and this fraction could be attributed to the presence of spores at the start of inactivation. Further heterogeneity within the vegetative cell population of strain ATCC 10987 could not be statistically validated, as the biphasic logistic and Geeraerd models were sufficient to describe the data acceptably and further model complexity could not be substantiated. The presence of spores at the start of inactivation was not observed for strain ATCC 14579. The existence of a heat-sensitive and a heat-resistant vegetative population was statistically acceptable for strain ATCC 14579 under most of the experimental conditions, although the parameter f was not significant. Reduction of the nonsignificant parameter f also resulted in redundancy of the parameter k_{res}, which was not statistically acceptable according to the F test. The presence of a mutated heat-resistant sub-

TABLE 3. Parameter estimates of the Geeraerd model

Strain	Growth phase	% NaCl	Parameter value[d]				
			$\log_{10} N(0)$	f	k_{sens}	t_S	k_{res}
ATCC 10987	Exponential	0	6.85	5.94×10^{-6}	5.65	NS	0[a]
		1	6.99	4.30×10^{-6}	0.71	NS	0[a]
		2.5	6.63	1.07×10^{-5}	0.62	NS	0[a]
		5	5.11	3.76×10^{-4}	1.06	NS	0[a]
	Transition	0	7.62	1.25×10^{-6}	0.71	1.73[c]	0[a]
		2.5	7.77	1.65×10^{-6}	0.55	NS	0[a]
	Stationary	0	7.73	2.60×10^{-6}	0.41	NS	0[a]
		2.5	7.39	1.72×10^{-5}	0.61	5.68	0[a]
ATCC 14579	Exponential	0	7.05	2.10×10^{-3}	0.77	NS	0.21
		1	6.92	1.22×10^{-3}[b]	0.91	8.87	0.27
		2.5	6.70	3.30×10^{-4}[b]	0.57	9.07	0.14[b]
		5	6.49	6.89×10^{-4}[b]	0.63	5.88	0.17
	Transition	0	7.86	8.40×10^{-5}[b]	0.47	6.76	0.12
		2.5	7.95	NS	0.35	13.52	NS
	Stationary	0	8.13	1.27×10^{-4}[b]	0.35	NS	0.09
		2.5	8.07	1.94×10^{-3}[b]	0.49	5.20	0.15

[a] Parameter was fixed at 0 because the inactivation rate k_{res} was 0 for the heat-resistant population of spores at 50°C.
[b] Parameter was not significant for this experimental condition, but the parameter was not excluded from the model because the F test showed that the phenomenon of two populations was significant.
[c] Parameter was significant ($P = 0.01$) when the model was fitted to all the replicate data together for this experimental condition. When replica curves were fitted individually, the average parameter estimate was not statistically significant ($P = 0.14$).
[d] NS, nonsignificant parameter for this experimental condition.

population of vegetative cells for strain ATCC 14579 was evaluated by collecting colonies at the time points corresponding to the end of the inactivation curvatures. Cell suspensions obtained from these colonies did not exhibit enhanced thermotolerance compared to the original inactivation curves, indicating that the biphasic curvature was not caused by the presence of a genetically more resistant vegetative subpopulation. Furthermore, in addition to the presence of a fraction of spores, a stable heat-resistant subpopulation of vegetative cells could not be demonstrated experimentally for strain ATCC 10987 either.

Quantification of effects of salt stress and physiological state on thermotolerance. After selection of the biphasic logistic model and the Geeraerd model as the most suitable models and reduction of the number of parameters for some experimental conditions, the parameter estimates of these models were used to compare the different experimental conditions. The replicate experiments for each condition were fitted individually with the reduced biphasic logistic and reduced Geeraerd models. The average parameter estimates were statistically compared using analysis of variance and t tests. The results of the t tests are shown in Tables 4 and 5. P values shown refer to statistical analyses using the Geeraerd model.

The preexposure of exponential-phase cells to salt resulted in an adaptive response rendering the exponential-phase cells more resistant to heat, and the largest increase in heat resistance of exponential-phase cells was achieved after preexposure to 2.5% salt (Tables 2 and 3). At this concentration, strain ATCC 10987 showed a nine times decreased inactivation rate compared to that for exponential-phase cells without salt preexposure. However, significant differences after preexposure to 1% and 5% salt could not be confirmed. Also, strain ATCC 14579 showed the lowest inactivation rate after preexposure to 2.5% salt and displayed the most extended shoulder period after this pretreatment. This inactivation rate was significantly lower than the inactivation rate after preexposure to 1% salt but not significantly different from the inactivation rate after preexposure to 5% salt. The shoulder period after preexposure to 2.5% salt was comparable to that after preexposure to 1% salt and was prolonged compared to that after preexposure to 5% salt. As a consequence, 2.5% salt was chosen to investigate the effects of salt preexposure on the heat resistance of transition- and stationary-phase cells.

The inactivation kinetics of transition- and stationary-phase cells revealed that the physiological state of the cells influenced the heat resistance of cells. Transition- and stationary-phase cells of strain ATCC 10987 exhibited enhanced resistance to heat compared to exponential-phase cells. Stationary-phase cells of strain ATCC 10987 appeared to be the most resistant, as reflected in the lowest inactivation rate. The heat resistance of strain ATCC 14579 was maximal for transition-phase cells. Transition-phase cells showed a significant shoulder period ($P = 0.01$) and a similar inactivation rate to that of stationary-phase cells.

TABLE 4. Comparison of parameter estimates of the Geeraerd model for *Bacillus cereus* ATCC 10987, using P values

Growth phase (% NaCl)[a]	P value for difference in k_{sens} values[b]							
	Exp (0)	Exp (1)	Exp (2.5)	Exp (5)	Trans (0)	Trans (2.5)	Stat (0)	Stat (2.5)
Exp (0)								
Exp (1)	**0.00**							
Exp (2.5)	**0.00**	0.22						
Exp (5)	**0.00**	0.08	0.07					
Trans (0)	**0.00**	0.44	0.26	0.09				
Trans (2.5)	**0.00**	**0.03**	0.15	0.05	0.11			
Stat (0)	**0.00**	**0.01**	**0.02**	**0.04**	**0.03**	**0.01**		
Stat (2.5)	**0.00**	0.48	0.34	0.08	0.44	0.18	0.06	

[a] Exp, exponential; trans, transition; stat, stationary.
[b] Bold values indicate that the two compared parameter estimates were significantly different according to the t test (one-sided).

TABLE 5. Comparison of parameter estimates of the Geeraerd model for *Bacillus cereus* ATCC 14579, using *P* values

Growth phase (% NaCl) and parameter[a]	*P* value for difference in parameter values[b]							
	Exp (0)	Exp (1)	Exp (2.5)	Exp (5)	Trans (0)	Trans (2.5)	Stat (0)	Stat (2.5)
k_{sens}								
Exp (0)								
Exp (1)	0.12							
Exp (2.5)	0.11	**0.01**						
Exp (5)	0.11	**0.00**	0.43					
Trans (0)	**0.01**	**0.00**	**0.04**	**0.01**				
Trans (2.5)	**0.00**	**0.00**	**0.00**	**0.00**	**0.01**			
Stat (0)	**0.01**	**0.00**	**0.02**	**0.01**	0.17	0.20		
Stat (2.5)	0.15	**0.04**	0.48	0.45	0.18	**0.04**	0.10	
t_s								
Exp (0)	NS							
Exp (1)	NS							
Exp (2.5)	NS	0.42						
Exp (5)	NS	**0.01**	**0.02**					
Trans (0)	NS	0.11	0.10	0.43				
Trans (2.5)	NS	**0.01**	**0.01**	**0.00**	**0.00**			
Stat (0)	NS	NS	NS	NS	NS	NS	NS	
Stat (2.5)	NS	**0.00**	**0.00**	0.50	0.41	**0.00**	NS	

[a] Exp, exponential; trans, transition; stat, stationary.
[b] Bold values indicate that the two compared parameter estimates were significantly different according to the *t* test (one-sided). NS, one of the two compared parameter estimates was a nonsignificant model parameter and was excluded from the model.

The adaptive response to salt was significantly influenced by the physiological state of the cells. Strain ATCC 10987 did not obtain enhanced thermotolerance by preexposure to 2.5% salt in the transition phase, but stationary-phase cells were a little more resistant after preexposure to salt, since a just significant shoulder period was observed ($P = 0.05$). Strain ATCC 14579 showed an adaptive response in both the transition and stationary phases, as a significantly enhanced shoulder period was observed in both phases ($P = 0.00$).

To compare the effects of the salt stress response and physiological state on thermotolerance, the thermotolerance of exponential-phase cells after preexposure to 2.5% salt was compared to the thermotolerance of transition- and stationary-phase cells without preexposure to salt. The effect of growth phase on thermotolerance was comparable to the maximum adaptive salt stress response in exponential-phase cells for both strains. Transition-phase cells of strain ATCC 10987 showed a thermotolerance comparable to that of exponential-phase cells after preexposure to 2.5% salt. Stationary-phase cells of strain ATCC 10987 were significantly more heat resistant than exponential-phase cells after preexposure to 2.5% salt. Transition-phase cells of strain ATCC 14579 showed maximum heat resistance and were slightly more resistant than exponential-phase cells after preexposure to 2.5% salt.

The reported fractions in Tables 2 and 3 show the estimated spore fractions in the exponential, transition, and stationary phases for strain ATCC 10987 at the start of inactivation. The observed levels of spores in the exponentially growing cultures of strain ATCC 10987 were similar for the four exponential-growth-phase conditions tested ($P = 0.97$). Spores were formed further at the end of the growth cycle, as the transition- and stationary-phase cultures exhibited significantly larger amounts of spores than the exponential-phase cultures ($P = 0.00$), with the highest level of spores found in the stationary-phase cultures.

DISCUSSION

A deliberate combination of preservation hurdles can be used to design nutritious, tasty, and microbially safe minimally processed foods, and quantitative risk assessment studies can be used to optimize the balance between food quality and microbial safety. In many studies, it has been shown that adaptation to a certain type of stress may protect cells against other severe homologous or heterologous stresses (e.g., see references 3, 4, 17, 22, and 28). Since nonstressed microorganisms are often used in quantitative risk assessment studies, preservation measures based on these data might not be sufficient to ensure the safety of processed food. Therefore, in this study the effect of salt stress on thermotolerance was quantitatively assessed by using microbial survival models which were adequate for fitting the survival characteristics of strains ATCC 10987 and ATCC 14579.

Experimental design and fitting performances of survival models. Considering the biological variation mentioned by Browne and Dowds (4), inactivation experiments were reproduced on three different days, and sampling was performed in duplicate. The observed variation between days was obvious and was reflected in the measuring error. The measuring error influenced the selection of a statistically accepted model and was represented in the *f* value. The higher the measuring error, the less complex a model has to be to describe the data acceptably. It is important to include this biological variation in the quantification, and therefore reproductions have to be performed to provide valuable information for quantitative risk assessment studies. In addition, the experimental procedure influences the inactivation curvatures, which necessitates an unambiguous description of the experimental process in order to compare the data to those in other studies and to evaluate the findings.

The models used in this study describe the various survival curvatures known for vegetative cells. Both the Baranyi model and the modified Gompertz model were used to describe the sigmoid curvature. The fitting performance of the modified Gompertz model was better than that of the Baranyi model and might be preferred when the experimental data do not show linear behavior in the mid-phase, as this results in a better description of the data.

The statistical analyses performed with the biphasic logistic model and the Geeraerd model resulted in similar conclusions. One striking difference was observed between the fitting performances of both models, namely, in the estimation of the parameter $\log_{10} N(0)$. When the shoulder period t_s was not significant in both models, the parameter $\log_{10} N(0)$ was estimated to be lower by the biphasic logistic model than by the Geeraerd model. Both models can fit a curvature without a shoulder period by selecting a t_s of 0. However, the shoulder curvature is not completely eliminated from the biphasic logistic model when $t_s = 0$, resulting in a lower estimation of $\log_{10} N(0)$.

Parameter *f* of the biphasic logistic and Geeraerd models was not significant for most of the experimental conditions

tested for strain ATCC 14579 but was not excluded from the models because the *F* test showed that the biphasic inactivation was significant (Tables 2 and 3). Also, the parameter k_{res} was not significant for one experimental condition for strain ATCC 14579 (exponential-phase cells with preexposure to 2.5% salt) but was not excluded. The confidence intervals of both parameters were large when the parameters were not significant but not excluded (data not shown). Zwietering et al. mentioned that parameters which are strongly correlated are difficult to estimate and have large confidence intervals (32). The correlation matrices of the experimental conditions revealed that parameters f and k_{res} were strongly correlated (>0.99) when both parameters were not significant and not excluded (exponential-phase cells with preexposure to 2.5% salt). The correlation between both parameters was lower (>0.94) when only parameter f was nonsignificant and not excluded. Parameters were less correlated (<0.90) when both parameters were significant (exponential-phase cells without preexposure to salt).

Effect of salt preexposure on thermotolerance. The sodium chloride concentrations used in this study were both nonlethal and lethal for strains ATCC 10987 and ATCC 14579 (Fig. 1; Tables 2 and 3). Preexposure to 5% sodium chloride resulted in a significant decrease in cells at the start of inactivation [$\log_{10} N(0)$]. When cells are exposed to lethal salt stress conditions, two phenomena can take place, namely, the inactivation of bacterial cells and the induction of an adaptive response in the surviving cells, and this agrees with observations in *Listeria monocytogenes* (19, 20). In our study, differences in the heat sensitivities of cells after preexposure to nonlethal and lethal salt stress conditions could not be confirmed, indicating that cells which are able to survive lethal stress conditions are still capable of demonstrating an adaptive stress response that might be comparable to the adaptive stress response of cells which are exposed to nonlethal stress conditions.

Increased thermotolerance by short-term preexposure of cells to salt was observed previously in *B. cereus* ATCC 14579 (22) and *B. cereus* NCIMB 11796 (4). Periago et al. showed an overlap in proteins induced by heat shock and salt stress exposure as well as induction of non-heat-shock-specific proteins during salt stress exposure (22). Several heat shock proteins induced during salt stress exposure belong to the group of chaperones and proteases, and these proteins act together to maintain quality control of cellular proteins (1). Increased production of heat shock proteins after salt stress exposure in *B. cereus* was also demonstrated by Browne and Dowds (4) and was observed in other bacilli as well (21, 23, 29). In addition to de novo protein synthesis during preexposure to salt, Periago et al. mentioned an increase in thermotolerance after preexposure to salt in the presence of chloramphenicol, indicating an alternative and complementary mechanism (22). It has been shown that compatible solutes such as glycine betaine can function as thermoprotectants in *Bacillus subtilis* (12).

Thermotolerance and adaptive stress response are affected by strain diversity, physiological state, and population heterogeneity. Strains ATCC 10987 and ATCC 14579 showed differences in thermotolerance. Consequently, the adaptive stress responses of both strains cannot be compared straightforwardly, as preexposure to salt resulted in a lower inactivation rate for strain ATCC 10987 and an additional shoulder period for strain ATCC 14579. Thus, it was not feasible to conclude which strain showed the maximum adaptive stress response.

Cells toward the end of the growth cycle appeared to be most resistant to thermal stress. Cells were highly sensitive to heat during the exponential growth phase and became more resistant to heat during the transition and stationary phases, as observed previously for *B. cereus* NCIMB 11796 (4) and for other bacteria (see, e.g., reference 18). Induction of a generalized stress response and additional physiological changes provide enhanced resistance for cells toward the end of the growth cycle (25). Moreover, the transient decline in pH of the culture during the growth cycle, reaching pH values of 7.2 and 6.5 in the exponential phase for *B. cereus* ATCC 10987 and the transition phase for *B. cereus* ATCC 14579, respectively (data not shown), may have contributed in the latter case to the enhanced stress resistance of these cells. As shown by Browne and Dowds (3), 40 min of exposure of exponential-phase cells of *B. cereus* NCIMB 11796 to pH 6.3 resulted in enhanced stress resistance. Our study has shown that the effect of physiological state on heat resistance was comparable to the maximum adaptive response to salt demonstrated in exponential-phase cells. This indicates that two different stresses may provide similar increased resistance levels.

A growth cycle-dependent effect of salt adaptation was observed for both *B. cereus* strains. These results are consistent with other studies, which examined differences in heat shock-induced thermotolerance for exponential- and stationary-phase cells (14, 19). In the current study, we quantified the adaptive stress response in three different growth phases in more detail and demonstrated that the significance of the adaptive stress response was strain and growth phase dependent.

The inactivation kinetics of both strains showed heterogeneous heat resistance within the population. The tailing of strain ATCC 10987 was explained by a minor fraction of spores present at the start of inactivation, and concealment of heat-resistant vegetative cells in the tail could not be confirmed. No spores could be detected at the start of inactivation for strain ATCC 14579. The biphasic nature of the inactivation curvature for strain ATCC 14579 suggested heterogeneity within the vegetative cell population. However, genotypic heterogeneity was not found by assessment of the thermotolerance of survivors from the end of the inactivation curvature. Other studies agree with our observation suggesting that tail survivors are not genotypically distinct (5, 13). The reported phenotypic biphasic inactivation might be of practical importance in processing because a subpopulation is able to display greater resistance than that of the majority of the population, which might influence the safety margin settings.

In conclusion, based on statistical indices and model characteristics, biphasic models with a shoulder period were selected. Both models could be used to quantify in detail the effect of salt stress response on thermal inactivation kinetics for exponential-, transition-, and stationary-phase cells of strains ATCC 10987 and ATCC 14579. Each model parameter was used to characterize a survival characteristic, and both models were flexible, allowing a reduction of parameters when certain phenomena were not present. Strain diversity had the greatest impact on thermotolerance and survival curvatures. The maximal adaptive salt stress response in exponential-phase

cells was comparable to the effect of physiological state on thermotolerance. The adaptive salt stress responses of transition- and stationary-phase cells were less pronounced than that of exponential-phase cells. Quantification of the adaptive stress response might be instrumental to understanding the adaptation mechanisms and might allow the food industry to develop more accurate and realistic quantitative risk assessments.

REFERENCES

1. **Abee, T., and J. A. Wouters.** 1999. Microbial stress response in minimal processing. Int. J. Food Microbiol. **50:**65–91.
2. **Baranyi, J., A. Jones, C. Walker, A. Kaloti, T. P. Robinson, and B. M. Mackey.** 1996. A combined model for growth and subsequent thermal inactivation of *Brochothrix thermosphacta*. Appl. Environ. Microbiol. **62:**1029–1035.
3. **Browne, N., and B. C. A. Dowds.** 2002. Acid stress in the food pathogen *Bacillus cereus*. J. Appl. Microbiol. **92:**404–414.
4. **Browne, N., and B. C. A. Dowds.** 2001. Heat and salt stress in the food pathogen *Bacillus cereus*. J. Appl. Microbiol. **91:**1085–1094.
5. **Buchanan, R. L., M. H. Golden, R. C. Whiting, J. G. Phillips, and J. L. Smith.** 1994. Non-thermal inactivation models for *Listeria monocytogenes*. J. Food Sci. **59:**179–188.
6. **Cerf, O.** 1977. Tailing of survival curves of bacterial spores. J. Appl. Bacteriol. **42:**1–19.
7. **Couvert, O., S. Gaillard, N. Savy, P. Mafart, and I. Leguérinel.** 2005. Survival curves of heated bacterial spores: effect of environmental factors on Weibull parameters. Int. J. Food Microbiol. **101:**73–81.
8. **Ehling-Schulz, M., M. Fricker, and S. Scherer.** 2004. *Bacillus cereus*, the causative agent of an emetic type of food-borne illness. Mol. Nutr. Food Res. **48:**479–487.
9. **Frankland, G. C., and P. F. Frankland.** 1887. Studies on some new microorganisms obtained from air. Philos. Trans. R. Soc. Lond. Ser. B Biol. Sci. **173:**257–287.
10. **Geeraerd, A. H., C. H. Herremans, and J. F. Van Impe.** 2000. Structural model requirements to describe microbial inactivation during a mild heat treatment. Int. J. Food Microbiol. **59:**185–209.
11. **Geeraerd, A. H., V. P. Valdramidis, and J. F. Van Impe.** 2005. GInaFiT, a freeware tool to assess non-log-linear microbial survivor curves. Int. J. Food Microbiol. **102:**95–105. (Erratum, in press.)
12. **Holtmann, G., and E. Bremer.** 2004. Thermoprotection of *Bacillus subtilis* by exogenously provided glycine betaine and structurally related compatible solutes: involvement of Opu transporters. J. Bacteriol. **186:**1683–1693.
13. **Humpheson, L., M. R. Adams, W. A. Anderson, and M. B. Cole.** 1998. Biphasic thermal inactivation kinetics in *Salmonella enteritidis* PT4. Appl. Environ. Microbiol. **64:**459–464.
14. **Jorgensen, F., T. B. Hansen, and S. Knochel.** 1999. Heat shock-induced thermotolerance in *Listeria monocytogenes* 13-249 is dependent on growth phase, pH and lactic acid. Food Microbiol. **16:**185–194.
15. **Larsen, H. D., and K. Jorgensen.** 1999. Growth of *Bacillus cereus* in pasteurized milk products. Int. J. Food Microbiol. **46:**173–176.
16. **Leistner, L., and L. G. M. Gorris.** 1995. Food preservation by hurdle technology. Trends Food Sci. Technol. **6:**41–46.
17. **Lou, Y., and A. E. Yousef.** 1996. Resistance of *Listeria monocytogenes* to heat after adaptation to environmental stresses. J. Food Prot. **59:**465–471.
18. **Martinez, S., M. Lopez, and A. Bernardo.** 2003. Thermal inactivation of *Enterococcus faecium*: effect of growth temperature and physiological state of microbial cells. Lett. Appl. Microbiol. **37:**475–481.
19. **McMahon, C. M. M., C. M. Byrne, J. J. Sheridan, D. A. McDowell, I. S. Blair, and T. Hegarty.** 2000. The effect of culture growth phase on induction of the heat shock response in *Yersinia enterocolitica* and *Listeria monocytogenes*. J. Appl. Microbiol. **89:**198–206.
20. **Pagan, R., S. Condon, and F. J. Sala.** 1997. Effects of several factors on the heat-shock-induced thermotolerance of *Listeria monocytogenes*. Appl. Environ. Microbiol. **63:**3225–3232.
21. **Periago, P. M., T. Abee, and J. A. Wouters.** 2002. Analysis of the heat-adaptive response of psychrotrophic *Bacillus weihenstephanensis*. Int. J. Food Microbiol. **79:**17–26.
22. **Periago, P. M., W. van Schaik, T. Abee, and J. A. Wouters.** 2002. Identification of proteins involved in the heat stress response of *Bacillus cereus* ATCC 14579. Appl. Environ. Microbiol. **68:**3486–3495.
23. **Petersohn, A., M. Brigulla, S. Haas, J. D. Hoheisel, U. Volker, and M. Hecker.** 2001. Global analysis of the general stress response of *Bacillus subtilis*. J. Bacteriol. **183:**5617–5631.
24. **Rasko, D. A., J. Ravel, O. A. Okstad, E. Helgason, R. Z. Cer, L. Jiang, K. A. Shores, D. E. Fouts, N. J. Tourasse, S. V. Angiuoli, J. Kolonay, W. C. Nelson, A. B. Kolsto, C. M. Fraser, and T. D. Read.** 2004. The genome sequence of *Bacillus cereus* ATCC 10987 reveals metabolic adaptations and a large plasmid related to *Bacillus anthracis* pXO1. Nucleic Acids Res. **32:**977–988.
25. **Samelis, J., and J. N. Sofos.** 2003. Strategies to control stress-adapted pathogens, p. 303–351. *In* A. E. Yousef and V. K. Juneja (ed.), Microbial stress adaptation and food safety. CRC Press, Boca Raton, Fla.
26. **Te Giffel, M. C., and M. H. Zwietering.** 1999. Validation of predictive models describing the growth of *Listeria monocytogenes*. Int. J. Food Microbiol. **46:**135–149.
27. **Van Gerwen, S. J. C., and M. H. Zwietering.** 1998. Growth and inactivation models to be used in quantitative risk assessments. J. Food Prot. **61:**1541–1549.
28. **Van Schaik, W., M. H. Tempelaars, J. A. Wouters, W. M. de Vos, and T. Abee.** 2004. The alternative sigma factor σ^B of *Bacillus cereus*: response to stress and role in heat adaptation. J. Bacteriol. **186:**316–325.
29. **Volker, U., H. Mach, R. Schmid, and M. Hecker.** 1992. Stress proteins and cross-protection by heat shock and salt stress in *Bacillus subtilis*. J. Gen. Microbiol. **138:**2125–2135.
30. **Whiting, R. C.** 1993. Modeling bacterial survival in unfavorable environments. J. Ind. Microbiol. **12:**240–246.
31. **Xiong, R., G. Xie, A. E. Edmondson, and M. A. Sheard.** 1999. A mathematical model for bacterial inactivation. Int. J. Food Microbiol. **46:**45–55.
32. **Zwietering, M. H., J. T. de Koos, B. E. Hasenack, J. C. de Wit, and K. van 't Riet.** 1991. Modeling of bacterial growth as a function of temperature. Appl. Environ. Microbiol. **57:**1094–1101.
33. **Zwietering, M. H., I. Jongenburger, F. M. Rombouts, and K. van 't Riet.** 1990. Modeling of the bacterial growth curve. Appl. Environ. Microbiol. **56:**1875–1881.